https://doi.org/10.46813/2023-145-012

CURVATURE OF THE DIFFRACTION CONE OF PROTON-PROTON ELASTIC SCATTERING AT HIGH ENERGIES IN MAXIMAL POMERON AND ODDERON MODEL

O. Lengyel[1],, N. Bence[2], I. Szanyi[3,4]*
[1]Institute of Electron Physics of NAS of Ukraine, Uzhhorod, Ukraine;
[2]Uzhhorod National University, Uzhhorod, Ukraine;
[3]Wigner RCP, POB 49, Budapest, 1525, Hungary;
[4]Eötvös University, Pázmány P. s. 1/A, Budapest, 1117, Hungary
**E-mail: alexanderlengyel39@gmail.com*

The values of the slope *B(s,t)* and curvature parameter *C(s,t)* have been calculated within the framework of the maximal Pomeron and Odderon approach in the wide *s*- and low *t*-range with the allowance made for the diffraction cone shape. The absolute values of the averaged curvature parameter *<C(s,t)>* is predicted to be decreasing depending on s and change of sign at asymptotically large energies far from achievable ones.

PACS: 13.85.DZ

INTRODUCTION

Concerning the search for “asymptopia” many years ago Jorge Dias de Deus and Antonio Braz de Padua [1] rightly argued: “At the moment, the situation is such that we do not find any evidence for new and not old-fashioned physics in hadronic diffraction at high energies. Odderon and threshold effects may be there, but do not seem to be relevant for the description of the bulk of the interactions: total cross-section, ratio ρ, differential cross-section, etc”. Many others think that we are still extremely far from the asymptopia, the region where some known asymptotic relations should hold. The time has come when you can reconsider these predictions. Now the ideal place to search for the asymptopia is the LHC [2–4].

1. CHOICE OF DATA

The Collider experiments on elastic *pp*-scattering brought us closer to answering the question where is asymptopia? In the elastic hadron-hadron scattering the fine structure parameters of diffraction cone such as the slope

$$B(s,t) = \frac{d}{dt}\left(\ln \frac{d\sigma(s,t)}{dt}\right) \qquad (1)$$

and curvature

$$C(s,t) = \frac{1}{2}\left(\frac{d}{dt}B(s,t)\right) \qquad (2)$$

considered as a sensitive indicator of the transition to asymptopia [5].

Recently it was found that the curvature effects while small, lead to significant changes in the forward slope parameter relative to that determined in purely exponential fit and concluded that the effect of curvature in the small $-t$ differential cross sections should be included in fits to new data [6]. Curvature has been studied previously at much lower energies [7].

In [8] we found that the non-exponential function entering to the Pomeron pole residue, as well as the non-linearity of its trajectory is strongly suggested by the data. As a result, one can observe that the curvature parameter has a tendency to decrease and change the sign in a remote TeV area. In this relation the idea arises to revise the elastic *pp*-scattering data for wide interval of *s* from ISR to LHC energies for diffraction cone within the framework of the maximal Pomeron (Froissaron) and Odderon model (FMO). Due to the unified approach in calculating the characteristics of slope and curvature parameter we shall predict their energy behavior. For this we have collect the data set of differential cross-section for *pp*-scattering where the non-exponential behavior of diffraction cone is clearly present in broad area of energy and appropriate interval of momentum transfer to select the most suitable form of this non-exponentiality.

Next we chose the best form of Pomeron and Odderon as well as Reggeons for description of selected data set choosing non-exponential pole residue contributions of Pomeron and Odderon. For the completeness of the fit, we also added the experimental data of $\sigma_{tot}(s)$ and $\rho(s)$ from compilation [9] at $t=0$ for $\sqrt{s} \geq 5$ GeV which are important to describe the mentioned data set.

To look for non-exponential behavior similar to that observed in the ISR [10, 11] and LHC [1, 2] we have separate those experimental data for *pp*-scattering which contains large number of experimental points, namely: at E_{cm} = 19.4 [10]; 23.5; 30.7; 44.7; 52.8; 62.5 GeV [11]; 8 [1] and 13 TeV [2].

Concerning the boundary of *t*-range taking into account the Coulomb-nuclear interference region of the diffraction in general this boundary not less than $|t|$ = 0.03 GeV^2. The opposite boundary for large $-|t|$ excluding the dip-bump region, namely $|t|$ = 0.85 GeV^2.

2. FMO APPROACH

The Maximal Pomeron (Froissaron) and Maximal Odderon approach (FMO) give a good description of all accessible pp- and $\bar{p}p$ –elastic scattering at GeV and TeV energies and wide momentum transfer [13, 14]. Let us recall that this is one of the few approximations in which all the basic requirements are taken into account, including both for the scattering forward of Froissart theorem and the Auberson-Kinoshita-Martin theorem for $t \neq 0$. Taking into account the latest data from LHC [4], to describe the selected dataset, it is necessary to take into account not only the Pomeron, but also the contribution of the Odderon. The Pomeron contribution to the scattering amplitude in this case is:

$$P\left(s,t\right)=P_0\left(s,t\right)+P_1\left(s,t\right)+P_2\left(s,t\right). \quad (3)$$

The simple and dipole Pomerons have a conventional form:

$$P_0\left(s,t\right)=-\ a_{P,0}\tilde{s}^{\alpha_P(t)}e^{\varphi^{P}{}_0(t)}, \quad (4)$$

$$P_1\left(s,t\right)=-a_{P,1}\tilde{s}^{\alpha_P(t)}e^{\varphi^{P}{}_1(t)}\ln\tilde{s}, \quad (5)$$

$$\tilde{s}=\ -i\frac{s-2m^2}{2m^2}, \quad (6)$$

$$\alpha_p(t)=1+\alpha_p^{'}t, \quad (7)$$

while the tripole term has the form

$$P_2\left(s,t\right)=\tilde{s}a_{p,2}\frac{2J_1(z_p)}{z_p}e^{\varphi^{P}{}_2(t)}\ln^2\tilde{s} \quad (8)$$

according the AKM asymptotic theorem,

$$z_p=r_p\tau\ln\ \tilde{s}, \quad (9)$$

$$\tau=\sqrt{-t/t_0},\ t_0=1\ \text{GeV}^2. \quad (10)$$

The common form of residue functions suggests the non-linear exponent:

$$\varphi_{p,i}(t)=\beta_i^p\left(\sqrt{t_p}-\sqrt{t_p-t}\right), \quad (11)$$

$$t_p=4m_\pi^2. \quad (12)$$

Contribution of Odderon reads as:

$$O\left(s,t\right)=O_0\left(s,t\right)+O_1\left(s,t\right)+O_2\left(s,t\right), \quad (13)$$

$$O_0\left(s,t\right)=ia_{O,0}\tilde{s}^{\alpha_O(t)}e^{\varphi^{pO}{}_0(t)}, \quad (14)$$

$$O_1\left(s,t\right)=ia_{o,1}\tilde{s}^{\alpha_O(t)}e^{\varphi^{O}{}_1(t)}\ln\tilde{s}, \quad (15)$$

$$O_2\left(s,t\right)=i\tilde{s}a_{O,2}\frac{2J_1(z_O)}{z_O}e^{\varphi^{O}{}_2(t)}\ln^2\tilde{s}, \quad (16)$$

$$\varphi_i^O\ (t)=\beta_i^O\left(\sqrt{t_o}-\sqrt{t_o-t}\right), \quad (17)$$

$$t_O=9m_\pi^2, \quad (18)$$

$$\alpha_O(t)=1+\alpha_O^{'}t, \quad (19)$$

$$z_O=r_O\tau\ln\ \tilde{s}. \quad (20)$$

Contributions of the secondary Reggeons, f and ω have a standard form

$$R_1^{(f)}(s,t)=-g_1^{(f)}\tilde{s}^{\alpha_f(t)}e^{\varphi_1^{(f)}(t)}, \quad (21)$$

$$\alpha_f(t)=1+\alpha_f' t, \quad (22)$$

$$R_1^{(\omega)}(s,t)=-g_1^{(\omega)}\tilde{s}^{\alpha_\omega(t)}e^{\varphi_1^{(\omega)}(t)}, \quad (23)$$

$$\alpha_\omega(t)=1+\alpha_\omega' t. \quad (24)$$

In this model we use the following normalization of the total amplitude:

$$A_{\bar{p}p}^{pp}(s,t)=P\left(s,t\right)+R_1^{(f)}(s,t)\pm\left(\left(O\left(s,t\right)+R_1^{\omega}(s,t)\right)\right), \quad (25)$$

$$\frac{d\sigma}{dt}=\frac{1}{16\pi ks^2}\left|A_{\bar{p}p}^{pp}(s,t)\right|^2, \quad (26)$$

$$\sigma_t(s)=\frac{1}{s}ImA_{pp}^{\bar{p}p}(s,t=0), \quad (27)$$

$k = 0.38938$ mb·GeV^2, and

$$\rho(s)=\frac{ReA_{pp}^{\bar{p}p}\left(s,t=0\right)}{ImA_{pp}^{\bar{p}p}\left(s,t=0\right)}. \quad (28)$$

Table 1

Parameters of Simplified Froissaron and Maximal Odderon model

Pomeron contribution			
Parameter	Dimension	Value	Error
$g_{1,p}^{(S)}$	mb	44.536	0.907
$g_{1,p}^{(D)}$	mb	-2.7191	0.1552
$g_{1,p}^{(T)}$	mb	0.34725	0.00631
α'_P, GeV^{-2}	GeV^{-2}	0.57380	0.0274
r_p	GeV^{-1}	0.29450	0.00153
$\beta_{1,p}^{(S)}$	GeV^{-1}	2.4211	0.1775
$\beta_{1,p}^{(D)}$	GeV^{-1}	6.1907	0.2159
$\beta_{1,p}^{(T)}$	GeV^{-1}	5.6113	0.0995
Odderon contribution			
Parameter	Dimension	Value	Error
$g_{1,o}^{(S)}$	mb	-4.716	0.4822
$g_{1,o}^{(D)}$	mb	1.0319	0.0924
$g_{1,o}^{(T)}$	mb	-5.3758	0.0493
α'_o, GeV^{-2}	GeV^{-2}	0.68863	0.43704
r_o	GeV^{-1}	0.24139	0.02795
$\beta_{1,o}^{(S)}$	GeV^{-1}	0.000	fix at lim.
$\beta_{1,o}^{(D)}$	GeV^{-1}	1.3180	1.9230
$\beta_{1,o}^{(T)}$	GeV^{-1}	7.5320	1.4536
Reggeons contribution			
Parameter	Dimension	Value	Error
$g_1^{(f)}$	mb	41.725	4.104
$\alpha_f(0)$		0.43681	0.03528
$\alpha_f^{'}$	GeV^{-2}	0.8	fix at lim.
$b_1^{(f)}$	GeV^{-2}	17.402	5.215
$g_1^{(\omega)}$	mb	32.369	2.821
$\alpha_\omega(0)$		0.30355	0.0417
$\alpha_\omega^{'}$	GeV^{-2}	0.8	fix at lim.
$b_1^{(\omega)}$	GeV^{-2}	0.000	fix at lim.

Free parameters of the model were determined from the fit to the selected data. Results of the fits in considered model with $\chi^2/DOF = 1.16$ are shown in Table 1. Based on the foregoing, we can conclude that the simplified FMO model, taking into account the non-exponential form of the Pomeron and Odderon residue, gives a good description of the selected set of experimental data for the ISR and LHC energies and momentum transfer of diffraction cone.

3. CALCULATION OF SLOPE AND CURVATURE PARAMETER

Dependence of slope on t at various energies in the FMO model has a concave shape (Fig. 1).

Therefore in this case it is more convenient consider the slope $<B(s)>$ and curvature $<C(s)>$ averaged in some interval of $|t|$ [13].

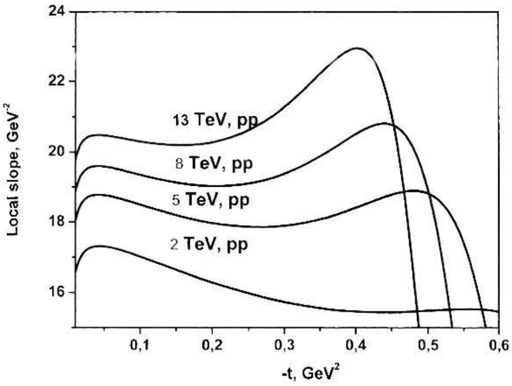

Fig. 1. Slope B(s,t) calculated in model

We did it in the intervals in accordance Table 2 for TeV energies.

$$< B(s) >= (1/\Delta_t)\left[\ln\left(\frac{d\sigma(t_{\min})/dt}{d\sigma(t_{\max})/dt}\right)\right], \quad (29)$$

where

$$\Delta_t = t_{mx} - t_{min}, \quad (30)$$

$$< C(s) >= (1/2\Delta)\big(B(t_{max}) - B(t_{min})\big) . \quad (31)$$

To calculate the slope B (t) at the points t_{max} and t_{min}, we use the formula for numerical differentiation:

$$B(s,t) = (1/2\Delta)\frac{\big(d\sigma(s,t+\Delta t) - d\sigma(s,t-\Delta t)\big)}{d\sigma(s,t)}. \quad (32)$$

The step was chosen as $\Delta_t = 10^{-6}$ GeV^2.

To calculate $<C(s)>$ according to the simplified MFO, the interval of momentum transfer with a descending branch of local slope *B (s, t)* should be selected (see Table 2 and Fig. 1).

Table 2

The boundaries for calculating the averaged curvature parameter in simplifies FMO model

Set	$\sqrt{s}$, GeV	$-t_{max}$, GeV	$-t_{min}$, GeV^2
ISR	19.4-62	0.030	0.850
LHC	8000	0.041	0.207
	13000	0.042	0.155

Within these boundaries the calculated averaged curvature shown in the Fig. 2 and has a decreasing character, which qualitatively corresponds to the behavior of the curvature determined directly from the experiment (squares). The value of curvature parameter depending on s changes its sign at asymptotically large energies.

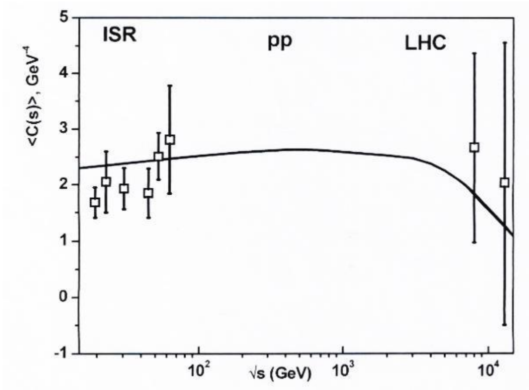

Fig. 2. Averaged curvature parameter calculated in simplifies FMO model (solid line). Open squares – "experimental" averaged curvature parameters. The bar represents the fitting uncertainty

The "experimental" averaged curvature parameter $<C(s)>$ calculated by Eqs. (28) with parameters obtained from the fit by the model of eq. (33) [7] for all selected sets of experimental data.

$$\frac{d\sigma(t)}{dt} = \mathrm{a}e^{\delta t + \gamma\sqrt{t_0 - t}}, \quad (33)$$

where $t_0 = 4m_\pi^2$.

4. CONCLUSIONS

We have studied the phenomenology of the pp-elastic scattering within both GeV and TeV energy range by using a model in which the analytical properties of the scattering amplitude are accounted for by the threshold singularity in the cross-channel. It has been shown that such features reflect adequately the "non-exponential" part of the t-dependence of the differential cross-section. To do this we have explored the FMO model, which naturally consider the curvature as the manifestation of the threshold structure of the scattering amplitude required by t-channel unitarity. The scattering amplitude represented by Froissaron, Maximal Odderon as well as by standard reggeons contributions was able to describe not only the total cross section and rho [12], but also the existing experimental data on differential [13] cross section and polarisation of pp- and $\bar{p}p$-scattering [14]. We emphasize that the non-exponential functions $\varphi(t)$ entering to in the Pomeron and Odderon pole residue are strongly suggested by the data. As a result, one can observe that the averaged curvature $<C(s)>$ behavior is predicted within the simplified maximum Pomeron and Odderon (FMO) model that satisfies the basic principles and has a tendency to decrease and change the sign in a area of hundreds TeV (see Fig. 2). It means that the "asymptopia" lies in a distant area.

REFERENCES

1. Jorge Dias de Deus and Antonio Beaz de Padua. The search of asymptotia in soft physics at high energy // *Phys. Let. B.* 1993, v. 317, p. 428-432.
2. G. Antchev et al. (TOTEM Collaboration). Evidence of non-exponential elastic proton-proton differential cross-section at low |t| and √s =8 TeV by TOTEM // *Nucl. Phys. B.* 2015, v. 899, p. 527-546.
3. G. Antchev et al. (TOTEM Collaboration). Elastic differential cross-section measurement at $\sqrt{s}=$13 TeV by TOTEM // *Eur. Phys. J. C.* 2019, v. 79, p. 861.
4. G. Antchev et al. (TOTEM Collaboration). First determination of the ρ parameter at √s = 13 TeV – probing the existence of a colorless three-gluon bound state // *Eur. Phys. J. C.* 2019, v. 79, p. 785.
5. M.M. Block, B.N. Cahn. High-energy pp and $\bar{p}p$ forward elastic scattering and total cross sections // *Rev. Mod. Phys.* 1985, v. 57, p. 563.
6. M.M. Block, L. Durand, P. Ha, F. Halzen. Slope, curvature, and higher parameters in pp and $p\bar{p}$-scattering, and the extrapolation of measurements of $d\sigma(s,t)/dt$ to $t\ = 0$ // *Phys. Rev. D.* 2016, v. 93, p. 114009.
7. P. Desgrolard, J. Kontros, A.I. Lengyel, E.S. Martinov. Local nuclear slope and curvature in high energy pp- and $\bar{p}p$-elastic scattering // *Nuovo Cim.* 1997, v. 110A, p. 615.
8. N. Bence, I. Szanyi, A. Lengyel. Fine structure of the proton-proton and antiproton-proton diffraction cone at LHC energies // *Journal of Physical Studies.* 2022, v. 26, p. 1101.
9. Compilation https:// www.hepdata.net.
10. A. Schiz et al. High-statistics study of $\pi+p$, $\pi-p$, and pp elastic scattering at 200 GeV/s *// Phys. Rev. D.* 1981, v. 24, p. 26.
11. G. Barbiellini et al. Small-angle proton-proton elastic scattering at very high energies (460 GeV^2<s<2900 GeV^2) // *Phys. Lett. B.* 1972, v. 39, p. 663.
12. Evgenij Martynov, Basarab Nicolescu. Did TOTEM experiment discover the Odderon? // *Phys. Let. B.* 2018, v. 778, p. 414.
13. Evgenij Martynov, Basarab Nicolescu. Odderon effects in the differential cross-sections at Tevatron and LHC energies // *Eur. Phys. J. C.* 2019, v. 79, p. 461.
14. N. Bence, A. Lengyel, Z. Tarics, E. Martynov, G. Tersimonov. Froisaaron and Maximal Odderon with spin-flip in pp and $\bar{p}p$ high energy elastic scattering // *Eur. Phys. J. A.* 2021, v. 57, p. 265.

Article received 14.04.2023

КРИВИЗНА ДИФРАКЦІЙНОГО КОНУСА ПРОТОН-ПРОТОННОГО ПРУЖНОГО РОЗСІЯННЯ ПРИ ВИСОКИХ ЕНЕРГІЯХ У МОДЕЛІ МАКСИМАЛЬНОГО ПОМЕРОНА ТА ОДДЕРОНА

О. Лендел, Н. Бенце, І. Сані

Нахил $B(s,t)$ та параметр кривизни $C(s,t)$ розраховані у рамках моделі максимального Померона та Оддерона у широкому діапазоні s і при малих t з урахуванням форми дифракційного конуса. Передбачається, що абсолютне значення усередненого параметра кривизни $<C(s,t)>$ спадає залежно від s і змінює знак при асимптотично високих енергіях, далеких від досяжних.